Single-cell RNA-sequencing of stria vascularis cell types in the *Slc26a4*$^{-/-}$ mouse

Jin-Young Koh, **Corentin Affortit**, Paul T. Ranum, Cody West, William D. Walls, Hidekane Yoshimura, Jian Q. Shao, Brian Mostaert, Hela Azaiez, and Richard J.H. Smith

corentinaugustepierre-affortit@uiowa.edu

Molecular Otolaryngology & Renal Research Laboratories, University of Iowa, Iowa City, IA, USA

Introduction:

The *SLC26A4* gene encodes the anion exchanger Pendrin. In the inner ear, pendrin is expressed in the epithelial cells and transports bicarbonate (HCO3−) into the endolymph to maintain endolymphatic pH homeostasis. Lack of pendrin in *Slc26a4*$^{-/-}$ mice results in hearing loss, vestibular dysfunction, and an enlarged vestibular aqueduct. One of the primary pathological alterations is acidification of the endolymphatic pH. However, the contribution of the stria vascularis cell types in maintaining endolymphatic pH remains poorly characterized. We aimed to identify pH regulators in pendrin-expressing cells that contribute to homeostasis of endolymph pH and to define the pathogenic mechanisms that contribute to the dysregulation of endolymph pH in *Slc26a4*$^{-/-}$ mice.

Methods:

We conducted single-cell RNA sequencing of stria vascularis cells isolated from wild-type (WT) and *Slc26a4*$^{-/-}$ mice. Bioinformatic clustering analysis based on single-cell gene expression defined the different cell types within the stria vascularis. Gene Ontology (GO) enrichment analysis was performed on pendrin-expressing cells. Additionally, we investigated gene expression changes in *Slc26a4*$^{-/-}$ mice. Specific findings were confirmed at the protein level by immunofluorescence in *Slc26a4*$^{+/+}$ and *Slc26a4*$^{-/-}$ adult mice.

Single-cell isolation and unbiased clustering of the cochlear stria vascularis

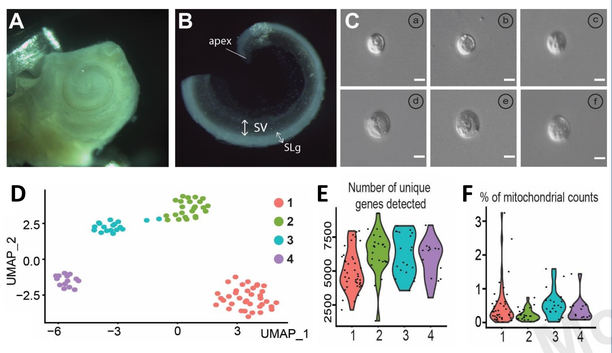

Figure 1: Single-cell isolation and unbiased clustering of the cochlear stria vascularis.
A-B: Picture of mouse cochlea (**A**) and isolated stria vascularis (**B**). The bony labyrinth is opened at the apex to access the membranous labyrinth (SV, stria vascularis; SLg, spiral ligament). **C**: Representative picture of isolated single cells. Note, the varied morphology. (**a**), (**b**) and (**c**) are Kcnj10-expressing cells. (**d**), (**e**) and (**f**) are Slc26a4-expressing cells. Scale bar: 10µm. **D**: UMAP clustering displays four distinct clusters (group 1, pink; 2, green; 3, cyan; 4, purple). **E-F**: Violin plot showing the number of unique genes detected per cell (**E**), and the percentage of mitochondrial counts (**F**). Each dot represents an individual cell. **Note:** These results suggest that the cell quality was excellent.

Clustering of the stria vascularis cells types

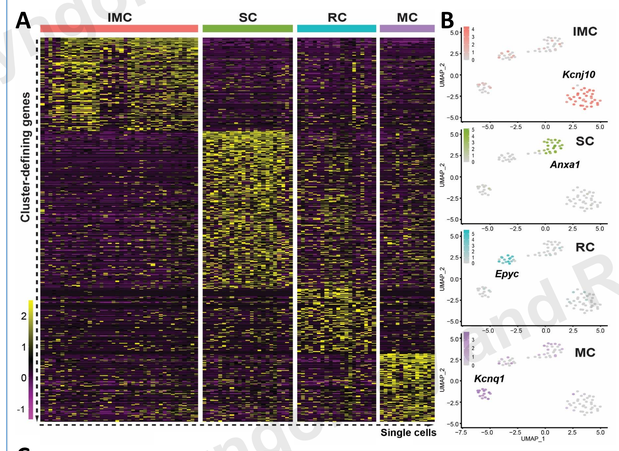

Figure 2: Clustering of the stria vascularis cells types.
A: Heatmap showing cluster-defining genes in intermediate cells (**IMC**), spindle cells (**SC**), root cells (**RC**), and marginal cells (**MC**). Each cell group's cluster-defining genes are ranked by ROC AUC score. **B:** The feature plot of each cell type show the expression of marker genes (IMC, Kcnj10; SC, Anxa1; RC, Epyc; MC, Kcnq1). **C:** Venn diagram showing the number of shared and unique genes for each cell type

Cluster-defining genes of the stria vascularis cells

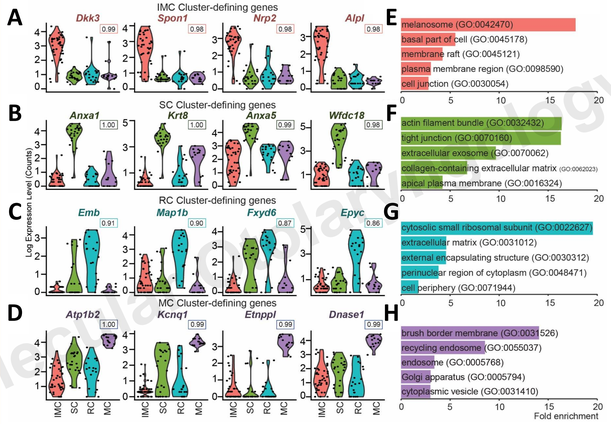

Figure 3: Cluster-defining genes of the stria vascularis cells.
A-D: Violin plots of the cluster-defining genes, including canonical marker genes. **A:** IMC (Dkk3, Spon1, Nrp2, Alpl); **B:** SC (Anxa1, Krt8, Anxa5, Wdc18); **C:** RC (Emb, Map1b, Fxyd6, Epyc); **D:** MC (Atp1b2, Kcnq1, Etnppl, Dnase1). The ROC AUC score of each gene is indicated under the name of the gene. **E-H:** Selected enriched Gene Ontology (GO) in the IMC (**E**), SC (**F**), RC (**G**), and MC (**H**). **Note:** The melanosome, plasma membrane, membrane raft, and cell junction genes are enriched in the IMC; the SC expresses components of the extracellular exosome, the extracellular matrix is enriched in the RC, and the recycling endosome and Golgi apparatus are enriched in the MC. (IMC, pink; SC, green; RC, cyan; MC, purple).

pH regulators of the spindle cell

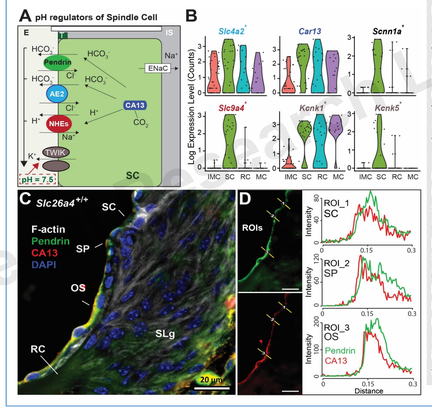

Figure 4: pH regulators of the spindle cell.
A: Schematic model of pH regulation in the SC. Endolymph pH is maintained by pendrin (Cl−/HCO3−) and by AE2, NHEs, TWIK, together with carbonic anhydrase (CA13) and ENac. **B:** Violin plot showing the gene expression of pH regulators, including anion exchangers. **C-D:** Representative confocal images of transversal cochlea section showing the colocalization of pendrin (green) and CA13 (red). OS, outer sulcus; RC, root cells; SC, spindle cells; SLg, spiral ligament; SP, spiral prominence; blue, nuclei; grey, F-actin. **D:** Diagram showing the line analysis (Y-axis, fluorescence intensity; X-axis, distance along the region of interest (ROI)).

Alteration of Anxa1 localization in the stria vascularis of the Slc26a4$^{-/-}$ *mice*

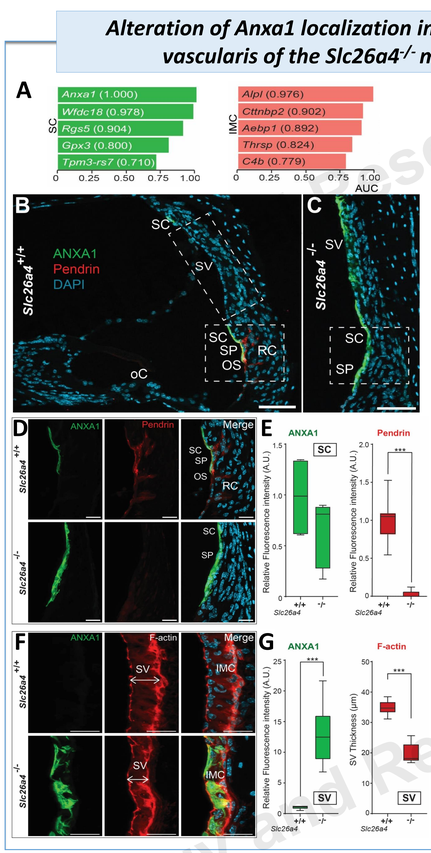

Figure 5: Alteration of Anxa1 localization in *Slc26a4*$^{-/-}$ mice.
A: Rank-ordered pH-dependent genes based on ROC AUC score. **B-C:** Representative confocal images of *Slc26a4*$^{+/+}$ and *Slc26a4*$^{-/-}$ mice aged 1 month, with ANXA1 (green), pendrin (red), and nuclei (cyan). Scale bar: 50µm. (oC, organ of Corti; OS, outer sulcus; RC, root cells; SC, spindle cells; SP, spiral prominence. **D:** High magnification of B-C. **Note:** In *Slc26a4*$^{+/+}$ mice, ANXA1 expression co-localizes with pendrin in the apical membranes of the SC. In contrast, in *Slc26a4*$^{-/-}$ mice, the area of the ANXA1 positive cells is expanded. **E:** Box plot showing the relative fluorescence intensity of pendrin and ANXA1 in SCs. **F:** Representative confocal images of the SV with ANXA1 (green), F-actin (red), and nuclei (cyan). Scale bar: 20µm. **G:** Box plot showing the relative fluorescence intensity of ANXA1 in SV cells and SV thickness (***, p<0.0005). **Note:** ANXA1 is present in the SV of *Slc26a4*$^{-/-}$mice.

Increased AP-2 expression in Slc26a4$^{-/-}$*mice*

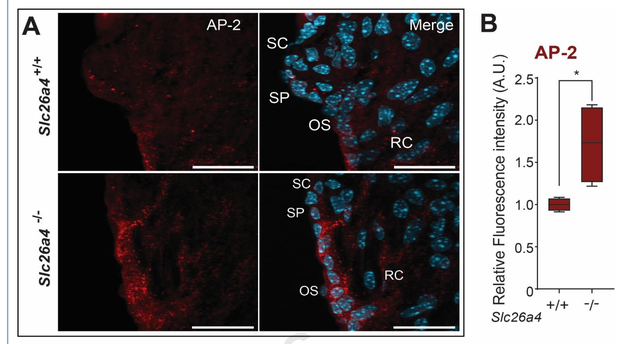

Figure 6: Increased adaptor protein 2 expression in *Slc26a4*$^{-/-}$ mice.
A: Representative images of the SC area form *Slc26a4*$^{+/+}$ and *Slc26a4*$^{-/-}$ mice aged 1 month, showing AP-2 (red) and nuclei (cyan). Scale bar: 20µm. (OS, outer sulcus; RC, root cells; SC, spindle cells; SP, spiral prominence). **B:** Box plot showing the relative fluorescence intensity of AP-2 in pendrin-expressing cells (*, p<0.005). **Note:** In *Slc26a4*$^{-/-}$ mice, AP-2 intensity increases in SC, SP, OS, and RC.

Increased IQGAP1 expression in Slc26a4$^{-/-}$*mice*

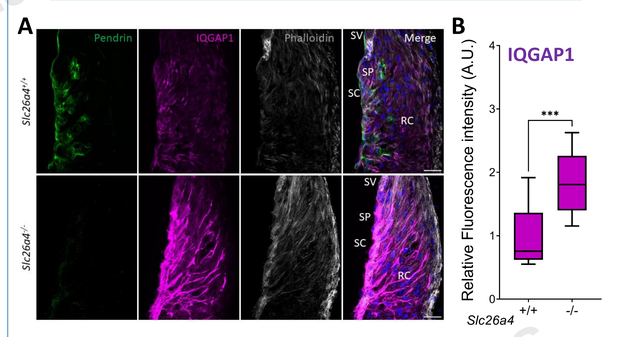

Figure 7: Increased IQGAP1 expression in Slc26a4$^{-/-}$ mice.
A: Representative images of the SC area form *Slc26a4*$^{+/+}$ and *Slc26a4*$^{-/-}$ mice aged 1 month, showing IQGAP1 (magenta), pendrin (green), phalloidin (grey) and nuclei (cyan). Scale bar: 20µm. (OS, outer sulcus; RC, root cells; SC, spindle cells; SP, spiral prominence; SV, stria vascularis). **B:** Box plot showing the relative fluorescence intensity of IQGAP1 in pendrin-expressing cells (***, p<0.0005).

Conclusion:

Single cell isolation of stria vascularis from *Slc26a4*$^{+/+}$ and Slc26a4$^{-/-}$ mice combined with transcriptomic analyses defined stria vascularis cell type transcriptome profiles and showed altered expression of both AP-2 and IQGAP1 in spindle cells and of Anxa1 in intermediate cells.

Koh et al. 2023. https://doi.org/10.1186/s12920-023-01549-0

Acknowledgements:

This project was supported in part by NIH-NIDCD grants DC002842, DC012049, and DC017955 (RJHS).